1. Supplementary Tables

Supplementary Table 1 | Phenotype of medaka YAP MO-injected embryos

Morpholinos	Host	Amount of MOs (ng)	Human YAP mRNA (pg)	Total survived	Normal (%)	Flat body (%)	Heart dislocation (%)
YAP TB MO	WT	4		34	0	91	85
	WT	2		43	28	53	42
	WT	4	200	33	88	9	12
YAP SB MO	WT	5		36	11	89	0
	WT	2.5		39	64	36	0
Control MO	WT	5		28	100	0	0

Injected embryos were scored at st.25 for a flattened body and heart dislocation as shown in Extended Data Figure 2c.

Supplementary Table 2 | Epiboly phenotype of medaka YAP MO-injected embryos

Morpholinos	Host	Amount of MOs (ng)	Human YAP mRNA (pg)	Total survived	Normal (%)	Slow epiboly (%)	Arrest of epiboly (%)
YAP TB MO	WT	5		29	0	24	76
	WT	2		31	10	90	0
	hir	2		45	11	62	27
	hir	2	200	39	67	28	5
YAP SB MO	*hir*	5		36	13	87	0
Control MO	WT	5		31	100	0	0

Host "*hir*" represents embryos from *hir* heterozygous crosses. Injected embryos were scored at st.17 for slow epiboly, and at st.22 for arrest of epiboly as shown in Figure 1b.

Supplementary Table 3 | Epiboly phenotype of zebrafish YAP/TAZ MO-injected embryos

Morpholinos	Host	Amount of MOs (ng)	Total survived	Normal (%)	Slow epiboly (%)	Arrest of epiboly (%)
ZFYAP/TAZ TB MO	WT	2	63	0	62	38
	WT	1	71	8	92	0
ZFYAP/TAZ SB MO	WT	3	67	8	92	0
Control MO	WT	3	59	100	0	0

Injected embryos were scored at 70% and 100% epiboly of control embryos for slow epiboly, and at the 10-somite stage for arrest of epiboly.

Supplementary Table 4 | Analysis of cell autonomy of the *hir* mutation by cell transplantation

Donor	Recipient	Target	Rescued (%)	Total (n)
WT	*hir*	Cuvier's duct	42	12
hir	WT	Cuvier's duct	39	119
WT	*hir*	lens and retina	100	5
WT	*hir*	retina only	20	21

Total (n) is embryos that had donor cells in the target tissue

Supplementary Table 5 | Primers used in this study

	Forward	Reverse
cDNA cloning:		
MFYAP	GAACAATGGATCCGAGCCAG	CTATAACCATGTGAGGAAGC
MFsox3	GCAGTGATCATTTAAAGTTGCCT	TCTGTTTTTTCTTCTCAGATGTG
MF70KDaFN1a	CCATGGCCGGTCGCAGCAGC	GGAAAAGGACTGCTGGGGTTCACA
MF70KDaFN1b	CTTTGTTCGTCTCCAAAATGACC	TCACTCTATATCCCGTCACA
MFARHGAP18	AAAGAGGAGAAGCAGTGAAACATGAGCCG CCACC	GCATTGTTTAGAGTTGATCCTCTGTAAT GGGTTGCTTA
Genotyping:		
Mutant	GCAAAGCCCTGCTCCAGTA	CTGTGAACCACAGAGCTCCA
WT	GCAAAGCCCTGCTCCAGTT	CTGTGAACCACAGAGCTCCA
qPCR:		
MFARHGAP18qPCR	AAGGTGCTTCGAGTTAAAACAGG	AGAGCCGTCATTTCCACTAGC
MF EF1α qPCR	TGCGGAGGAATCGACAAAAG	GTGATACCACGCTCACGCTC
SB morpholino evaluation:		
MFYAPSBMO evaluation	AACGCCGTGATGAACCCCA	CCTCTGCTGGTTCAAGGCAT
ZFYAPSBMO evaluation	CGGCCACCAGATCGTCCATG	AGAGCTTTACGTGGGTCCTG
ZFTAZSBMO evaluation	CTGACTTCTGGCGACATGGAC	CGGGTTGACGCTTTGTGCTT

Supplementary Table 6 | Morpholinos and siRNAs used in this study

Morpholinos	
MF YAP TB MO	TGCGAACTCTTTGCGGCCCGAAAAC
MF YAP SB MO	AGTGCTAGCCTGAGTTACAAAGAAG
ZF YAP TB	GATCCATGACTCCAGATAAAAGTAA
ZF YAP 5’UTR	CTCTTCTTTCTATCCAACAGAAACC
ZF YAP SB	AGCAACATTAACAACTCACTTTAGG
siRNAs	
#1 Human YAP1 stealth RNA	GCAACUCCAACCAGCAGCAACAGAU
#2 Human YAP1 stealth RNA	GGAAGGAGAUGGAAUGAACAUAGAA
#1 Dog YAP1 stealth RNA	UAUAUUUCUCCAUCCUGAGUCAUGG

2. Supplementary Video legends

Supplementary Video 1 | Formation of the eye by coordinated invagination of the lens and retina in WT Dorsal bright-field view, anterior up, between st.19 and st.23 (14 h duration). In WT, the nascent lenses and retina undergo coordinated morphogenesis to locate the lens properly in the eye.

Supplementary Video 2 | Dislocation of the lens in *hir* mutants Dorsal bright-field view, anterior up, between st.20 and st.24 (17 h duration). The mutant lens placodes dislocate, round up and migrate anteriorly where they loosely reattach to the retina.

3. Supplementary Discussion: ARHGAP18-related genes

Inactivation of ARHGAP18 alone is insufficient to produce a clear phenotype, but over-expression of ARHGAP18 rescues the *hir* mutant phenotype (Extended Data Fig.9b) probably by mimicking the function of multiple ARHGAP genes. It is possible that there is a degree of redundancy among ARHGAP genes. ARHGAP genes form a large gene superfamily; humans have 54 ARHGAP genes and many of them remain poorly characterized. We identified 66 ARHGAP genes in the medaka genome. Phylogenetic analysis identified 9 closely related ARHGAP18 paralogs in vertebrate lineages (Extended Data Fig.9c).

A screen of 40 human ARHGAP genes using siRNA knock-down in a human cell line revealed that four of the ARHGAP18 paralogs (ARHGAP28, 40, STARD13 and DLC1; note that ARHGAP6 was not tested) and less closely related ARHGAP23 showed similar phenotypes to ARHGAP18 inactivation suggesting that these ARHGAP18 paralogs might compensate for each other in an embryo with diverse cell types (Extended Data Fig.9d). Indeed, knock-out mice of ARHGAP6 and 28, both highly homologous to ARHGAP18, do not display any recognizable phenotype due to compensatory up-regulation of other ARHGAP genes[39,40]. Collectively, these observations strongly support our assumption of a high degree of genetic redundancy between ARHGAP18-related genes during early medaka development.

4. Supplementary Discussion: Why does the *hir* medaka mutant exhibit a unique flattened phenotype rather than a cell proliferation defect?

First, it appears that functional subdivision of YAP and its paralog, TAZ, differs among vertebrates. In medaka, tissue tension is regulated mainly by YAP and cell proliferation is regulated mainly by TAZ. Consequently, cell proliferation defects are minimized in YAP mutant medaka, allowing manifestation of the flattened phenotype. In zebrafish, however, YAP and TAZ are more equally involved in tissue tension and cell proliferation regulation; YAP;TAZ double mutants therefore exhibit more pronounced slow epiboly than single mutants, resulting in lethality soon after epiboly. Occasionally, zebrafish YAP;TAZ double mutants survived until the 20-somite stage and exhibited the flattened body phenotype (data not shown). In mice, YAP may carry out both functions as early YAP knock-out (KO) mouse embryos not only have cell proliferation defects, resulting in early lethality, but also an FN mutant-like phenotype (Morin-Kensicki et al., 2006). In contrast, TAZ KO mice do not have early cell proliferation defects. In *Drosophila*, loss-of-function of Yki, the single YAP/TAZ ortholog, compromises cell proliferation and does not allow the manifestation of other defects. Second, persistence of maternal YAP in medaka attenuates gastrulation defects that would otherwise terminate embryogenesis before body shape defects become apparent. Finally, loss-of-function analysis in the holistic context of an entire organism is advantageous in uncovering YAP function. YAP-deficient cells behave normally in WT embryos, as shown in our cell transplantation experiments. This might account for the absence of flattening or tissue dislocation in tissue- or organ-specific YAP KO mice.

5. Supplementary Figure 1: Full-scan of Western blots

Associated with Figure 2c

pMRLC

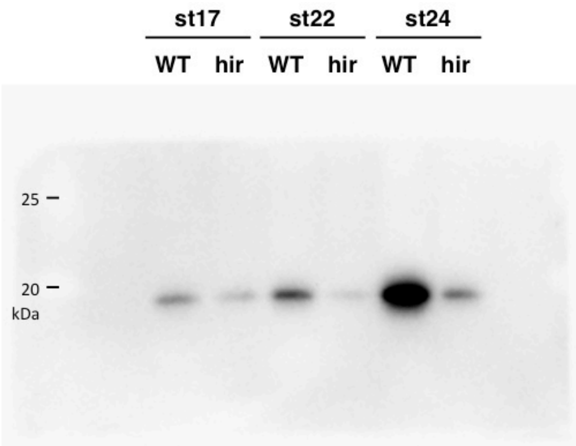

GAPDH

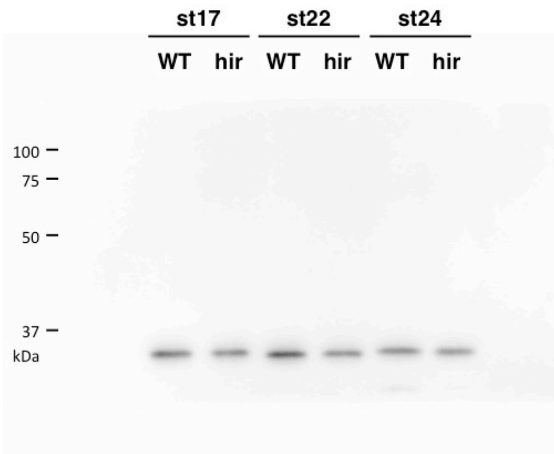

Associated with Figure 4c